Nonreciprocal Spin Wave Propagation in YIG/GGG: A Limit on the DMI Parameter

J. Trossman[*], Jinho Lim[†], and J. B. Ketterson

Department of Physics and Astronomy, Northwestern University, Evanston, IL 60208, USA

Wonbae Bang

School of Liberal Arts, Korea University of Technology and Education, Cheonan 31253, Korea

Materials with low damping, such as Yttrium Iron Garnet (YIG), are of interest in connection with spintronic devices. A promising structure for information storage is the Skyrmion, a domain wall quasi-particle. It has been shown that the stabilization of a Skyrmion can be energetically favorable with the addition of spin-orbit coupling (SOC) through the Dzyaloshinsky-Moriya Interaction (DMI). This interaction should be largest in metals, but still present in insulators. In order to produce spintronic devices using YIG, we must evaluate the DMI interaction inherent in the substrate used to grow the YIG, which is generally Gadolinium Gallium Garnet (GGG). In this paper, we measure nonreciprocal spin wave propagation in a thick YIG film in order to place a limit on the DMI parameter in a YIG/GGG bilayer.

Keywords: YIG, DMI

Email: wbang@koreatech.ac.kr

[*] Current address: Intel Corporation, Hillsboro, OR 97124, USA
[†] Current address: Materials Research Laboratory and Department of Materials Science and Engineering, University of Illinois Urbana-Champaign, Urbana, IL 61801, USA

I. INTRODUCTION

There has been much work recently directed toward the creation of spintronic devices [1-3], for the storage of information. One promising candidate is the Skyrmion [4-7], a topologically protected domain wall structure. The stabilization of Skyrmions can be facilitated by the Dzyaloshinsky-Moriya interaction (DMI), which arises from the antisymmetric part of the superexchange interaction [8-10] due to spin-orbit coupling and symmetry breaking. The Hamiltonian for this interaction was given by Dzyaloshinsky and Moriya [8, 9] as

$$H_{DMI} = \mathbf{D}_{ij}(\mathbf{S}_i \times \mathbf{S}_j), \quad (1)$$

where $\mathbf{D}_{ij}$ is a vector that points perpendicular to $\mathbf{r}_{ij}$, the vector from spin $\mathbf{S}_i$ to $\mathbf{S}_j$ and arises from symmetry breaking in the system.

In this paper, we focus on the interfacial DMI, in which the symmetry breaking is due to the interface between a ferromagnetic material and a spin-orbit coupled material. Therefore, the vector $\mathbf{D}_{ij}$ also lies in the plane of the interface. Contrary to exchange, which favors parallel or antiparallel spins, DMI prefers canted spins which precess around the vector $\mathbf{D}_{ij}$. In particular, DMI favors one direction of precession over the other, which leads to nonreciprocal spin wave dispersion [11-13], according to the theory of Moon et al. [14]. In addition, this interaction produces a nonreciprocal behavior of the attenuation of the spin waves as given in Eq. 2

$$\kappa = \frac{-pD^* + \frac{\rho_{ex}}{\mu} k_- \dfrac{2H + 4\pi M + 2\frac{\rho_{ex}}{\mu} k_-^2}{\sqrt{\left(H + \frac{\rho_{ex}}{\mu} k_-^2\right)\left(H + 4\pi M + \frac{\rho_{ex}}{\mu} k_-^2\right)}}}{pD^* + \frac{\rho_{ex}}{\mu} k_+ \dfrac{2H + 4\pi M + 2\frac{\rho_{ex}}{\mu} k_+^2}{\sqrt{\left(H + \frac{\rho_{ex}}{\mu} k_+^2\right)\left(H + 4\pi M + \frac{\rho_{ex}}{\mu} k_+^2\right)}}}, \quad (2)$$

where κ is the spin-wave amplitude ratio, p is ± 1 depending on the direction of the magnetic field, ρ_{ex} / μ is the exchange parameter, D^* is related to the amplitude of the DMI vector, $D^* = 2D / M$, and M is the saturation magnetization. Here, k_+ and k_- refer to the wave vectors associated with propagation on the two opposing sides of the film (GGG vs. free). Therefore, the spin-wave amplitude vs. field direction should differ for a nonzero D^*. The amplitude of the DMI vector, D, is larger in metals with the large atomic number Z and therefore much work has been done in systems using platinum [11, 13], but should be present in high-Z insulators as well.

In order to make spintronic devices with low losses, a material with small damping is desired. Yttrium Iron Garnet (YIG) is a ferromagnetic insulator with extremely low damping [15] (Gilbert damping $\alpha = 2.7 \times 10^{-5}$), which is generally grown on Gadolinium Gallium Garnet (GGG) for lattice matching purposes. Therefore, if devices are to be made out of YIG then the inherent DMI from the GGG must be taken into account.

II. EXPERIMENTS AND DISCUSSION

The experimental technique used here involves a direct measurement of the phase and amplitude of a propagating spin wave [16, 17]; a block diagram of the setup is shown in Fig. 1. A 5 mm × 5 mm sample of YIG 9.72 μm thick grown on GGG is pressed against a glass slide between two 50 μm wire antennas. A 25 dBm 6 GHz signal is applied through one of the antennas; the wave so launched is detected by the antenna on the opposing side. A portion of input amplitude, along with the output of the receive antenna, is applied to the input of a lock-in amplifier. The mixer output is proportional to the amplitude and phase difference between the input and output antennas which is, in turn, governed by the frequency and field dependence of the complex spin wavevector, k (f, H). The applied field, which varied between 1150 Oe to 1450 Oe, was modulated at 380 Hz to facilitate the lock-in detection. The lock-in output was recorded and averaged over multiple sweeps by a computer which also swept the magnetic field.

As we sweep the field, the lock-in output oscillates. A full oscillation corresponds to a 2π change in the phase, ϕ, which is given by, $\phi = kd$, where d is the path length in the film.

III. RESULTS

The sample is oriented in the Damon-Eshbach [18] geometry with the field perpendicular to the wavevector while in the plane of the sample. This mode exists on the low field side of the $k = 0$ mode, the ferromagnetic resonance (FMR). We obtain data in four configurations, one for each combination of forward and backward wavevector and field. The results are shown in Fig. 2, where we have selected an arbitrary direction to be positive. We note multiple oscillatory signals, one with large slowly oscillating amplitude and one with a smaller rapidly oscillating amplitude. This behavior arises from reflections of the spin wave at the sample edges. The large signal is the phase evolution of a spin wave that travels from the launching antenna to the receiving antenna. The small amplitude signal is due to the spin wave that is *reflected* from the receiving edge after which it undergoes a round trip to the receiving antenna. In the Damon-Eshbach mode, the surface wave is concentrated on one side of the sample depending on the field and wavevector directions. We note that for positive k / positive field configuration the spin wave is traveling on the *free side*, which is pressed up against a glass slide. Reversing either field or wavevector will flip the propagation to the *GGG side* of the YIG film. Reversing both returns the spin wave to the side pressed up against the glass slide, which we refer to as double reversal.

We observe the $k = 0$ mode, the ferromagnetic resonance, at around 1400 Oe. There is a small gap between the ferromagnetic resonance and the onset of coherent oscillations. This is likely due to the wavelength of the spin wave being longer than both the sample and antenna lengths; the wave fronts are then not strictly perpendicular to the sample's edge [19]. Therefore, the phase does not evolve in the manner described in section II until the spin-wave wavelength is safely smaller than the edge length of the sample.

The plots shown in Fig. 2 allow us to relate the field to the wavevector of the spin waves. Each oscillation corresponds to a change in the wavevector of $2\pi / d$ and so to find the absolute value of the wavevector, we fit the full Damon-Eshbach dispersion relation using the field position of the $k = 0$

mode. We note that due to the thickness of the sample, we are not in the linear regime of the dispersion relation, with k times the thickness of the sample as large as 0.5.

The amplitude of the spin waves as a function of wavevector is altered by geometric effects. Our sample was cut from a larger sample using a diamond saw which can introduce two effects. If the launching and receiving sides of our sample not parallel, there will be destructive interference since the antenna effectively integrates the arriving signal along the edge. The amplitude as a function of wavevector is then given by

$$\frac{1}{kl\sin\theta}\left[\sin(kd + kl\sin\theta) - \sin(kd)\right], \quad (3)$$

where is l is the length of the launching edge and θ is the angle between the launching edge and the receiving edge. We see that the amplitude should decrease as $1 / k$ and that the amplitude should have nodes where $kl\sin\theta = 2\pi$.

Edge roughness will introduce a random change δx in the path length traveled by the spin waves. If we approximate the roughness as sinusoidal, we find the amplitude as a function of k will involve a factor

$$\left|J_0(k\delta x)\right|, \quad (4)$$

which is oscillatory and decreasing with increasing k. Both of these effects are multiplicative factors that should be the same in both forward and backward propagating spin waves due to the symmetry of the system.

In order to examine nonreciprocity, we must compare either forward and backward propagating spin waves under a single direction of field or forward propagating spin waves under both directions of magnetic field. Fig. 2 shows a slight offset in our field readings depending on the direction of the field and so we will keep the field constant and examine the forward and backward propagating spin waves. An overlap of these plots is shown in Fig. 3. At first glance, these traces seem to be the same at the positive and negative fields and the spin wave dispersion appears identical up to the uncertainty of our measurement. Upon closer inspection, we observe a large difference in spin wave amplitude that scales with field and wavevector, consistent with Eq. 2. Additionally, we note a node in the amplitude at 1257 Oe, which may correspond to a node due to nonparallel edges or edge roughness. Since the spin wave dispersions at positive and negative fields are identical in Fig. 3, we do not discuss the overlay of forward and backward propagating spin waves with negative field more details.

Nonreciprocity has been examined in the past [20], and it was found through Brillouin light scattering (BLS) that for spin waves excited by a microstrip on top of a ferromagnet that the amplitude for forward and backward propagating Damon-Eshbach mode were vastly different. This measurement was done for wavevectors less than 100 cm^{-1}, which is commensurate with the wavevectors examined in this article. They note a much larger difference in amplitude than we observed. We believe that this difference arises due to the difference in excitation geometry.

If we attribute this difference in amplitude entirely to DMI, we can plot the ratio of backward to forward propagating spin waves. Under these assumptions, we can fit with Eq. 2 using a value for ρ_{ex} / μ of 6.2×10^{-9} Oe / cm^2, obtained from a separate measurement. From this fit, we find a value for the DMI parameter of $D = (-5.69 \pm 0.05) \times 10^{-4}$ mJ / m^2. This value is a relatively small number compared with an ultrathin YIG film [21], a CoPt film [22], a Permalloy film [23], and CoNi multilayers [24]. If we assume that DMI is the sole mechanism for the forward / backward amplitude asymmetry, then this value places a limit on the magnitude of the DMI parameter for the YIG / GGG interface.

IV. CONCLUSION

In this paper, we have used a phase-detection method to detect propagating spin waves in a YIG / GGG system. Using this method, we examined the propagation of spin waves in the forward and backward directions under positive and negative field. By examining the differences between forward and backward propagating spin waves under a positive field, we have placed a limit on the DMI interaction strength in a YIG / GGG system of $D = (-5.69 \pm 0.05) \times 10^{-4}$ mJ / m^2. To our knowledge, this is the first measurement of DMI in a fully insulating system.

ACKNOWLEDGEMENT

This research was carried out under support from the U.S. Department of Energy through grant DE-SC00144 at Northwestern, and Education and Research promotion program of KOREATECH in 2021 at Korea University of Technology and Education.

REFERENCES

[1] X. Yu, et al., Nat. Comm. **3**, 988 (2012)

[2] K. L. Wang, J. G. Alzate, and P. K., J. Phys. D: Appl. Phys. **46**(7), 074003 (2013)

[3] A. Hirohata and K. Takanashi., J. Phys. D: Appl. Phys. **47**(19), 193001 (2014)

[4] S. Rohart and A. Thiaville, Phys. Rev. B **88**(18), 184422 (2013)

[5] A. Fert, V. Cros, and J. Sampaio, Nat. Nanotech. **8**(3), 152 (2013)

[6] R. Tomasello, Sci. Rep. **4**, 6784 (2014)

[7] R. Wiesendanger, Nat. Rev. Mater. **1**(7), 16044 (2016)

[8] I. Dzyaloshinsky, J. Phys. Chem. Solids **4**(4) 241 (1958)

[9] T. Moriya, Phys. Rev. **120**(1), 91 (1960)

[10] A. Crpieux and C. Lacroix, J. Magn. Magn. Mater. **182**(3), 341 (1998)

[11] A. A. Stashkevich et al., Phys. Rev. B, **91**(21), 214409 (2015)

[12] K. Di et al., Appl. Phys. Lett. **106**(5), 052403 (2015)

[13] J. Lee et al., Nano Lett. **16**(1), 62 (2015)

[14] J. Moon et al., Phys. Rev. B **88**(18), 184404 (2013)

[15] B. Heinrich et al., Phys. Rev. Lett. **107**(6), 066604 (2011)

[16] J. Trossman et al., AIP Adv. **8**(5), 056024 (2018)

[17] X. Zhang et al., Phys. Rev. Lett. **113**(3), 037202 (2014)

[18] R. W. Damon and J. R. Eshbach, J. Phys. Chem. Solids **19**(3-4), 308–320, 1961

[19] S. O. Demokritov, B. Hillebrands, and A. N. Slavin, Phys. Rep. **348**(6), 441 (2001)

[20] T. Schneider et al., Phys. Rev. B **77**(21), 214411 (2008)

[21] H. Wang et al., Phys. Rev. Lett. **128**, 049902 (2022)

[22] Q. Zhang, et al., Phys. Rev. Lett. **128**, 167202 (2022)

[23] C. Hu, et al., Small, 2207206 (2023)

[24] J. Yu, et al., Sci Rep **6**, 32629 (2016)

Figure Captions.

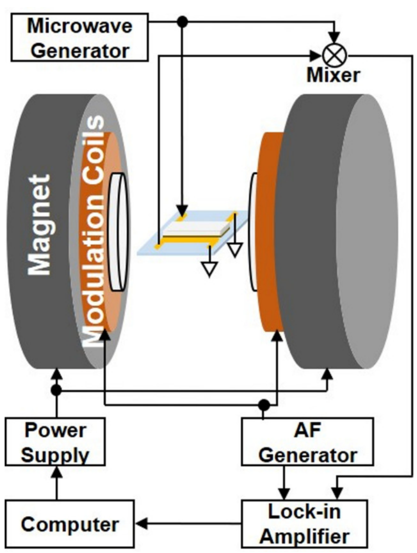

Fig. 1. A block diagram of the phase detection apparatus. A YIG sample is taped to the sample holder and placed inside a Varian electromagnet. A Hewlett Packer 8630 frequency synthesizer applies a 25 dBm microwave signal to one of two antennas running parallel to the sample edges with the other end grounded. The signal picked up by the second antenna is fed to a microwave mixer followed by a lock-in amplifier the output of which was recorded by a computer. The field is controlled by the current applied by two Kepco operational amplifier power supplies controlled by the computer. The field is

modualated at 380 Hz by a function generator and power amplifier which drives a pair of modulation coils. As the current in the main magnet is swept, the amplitude and phase of the transmitted signal changes and is recorded by the computer; the computer also sweeps the magnetic field.

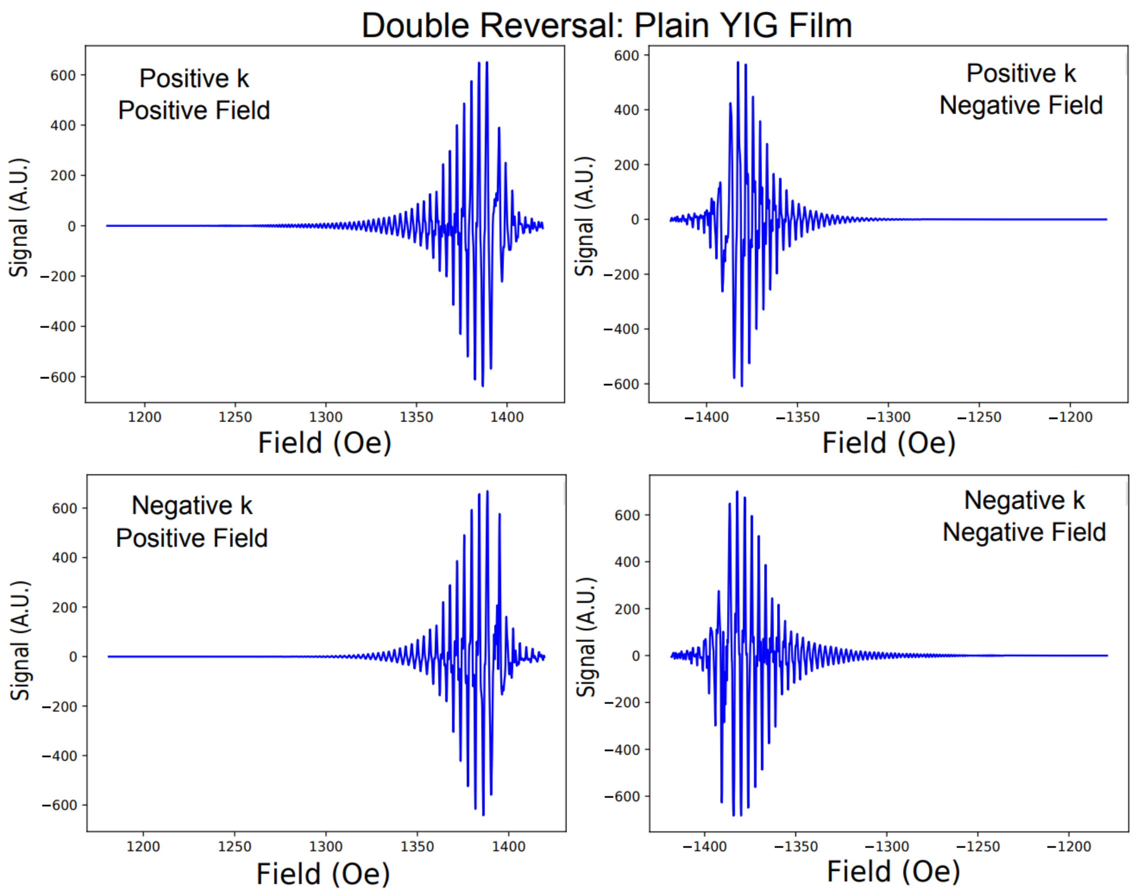

Fig. 2. Plots of the phase detection of Damon-Eshbach spin waves for four combinations of field direction and spin wave direction with respect to a control plot in the upper left. The sample is a bare YIG film pressed up against glass slide which means the structure is glass / air / YIG (9.72 μm) / GGG. Superficially, these plots look generally the same regardless of which field / wavevector combination is chosen. This is not completely the case as is shown in Fig. 3.

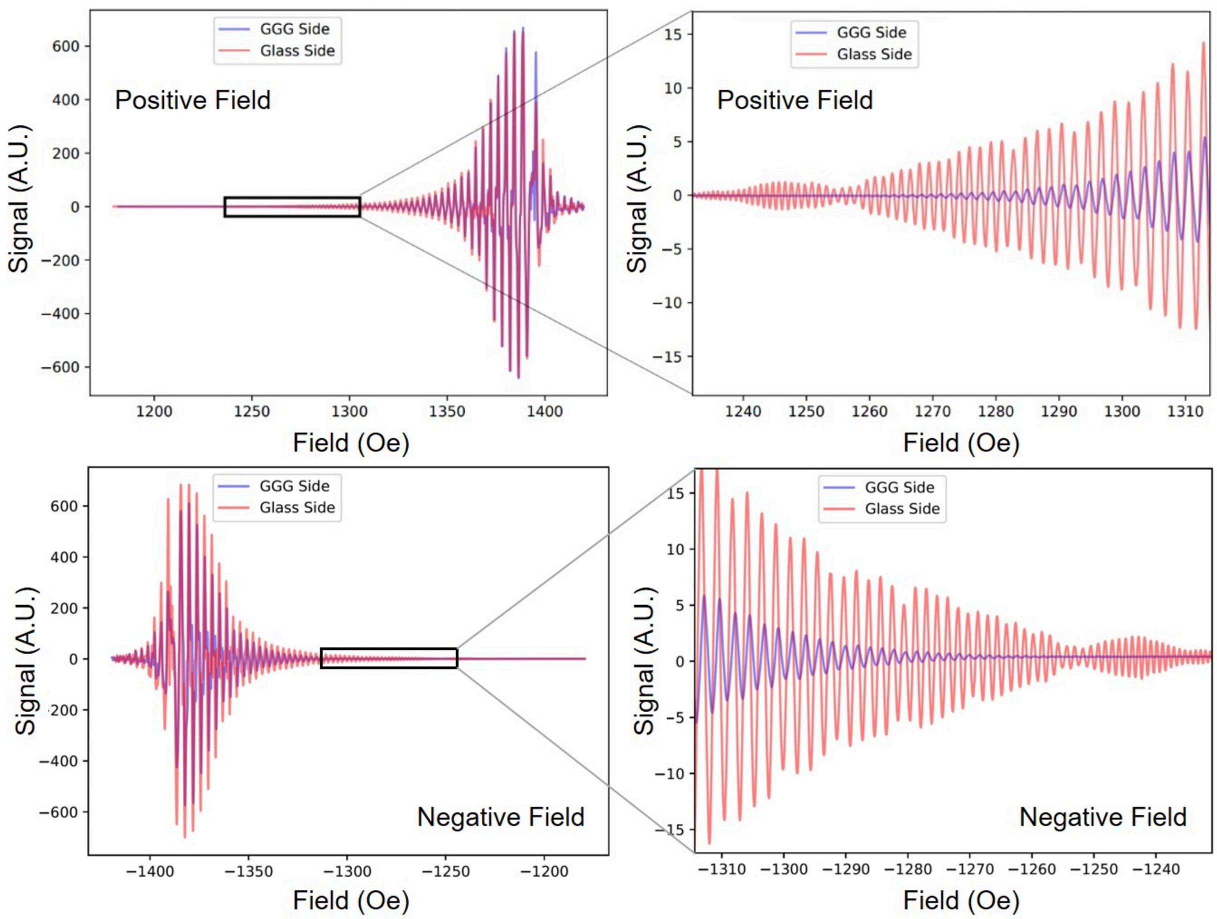

Fig. 3. Overlay of forward and backward propagating spin waves with positive and negative fields. While these plots look nearly identical when overlayed at both field sides, upon zooming in around 100 Oe from the FMR resonance field we see that the amplitude is vastly different. By taking the ratio of the amplitudes of the forward and backward propagating spin waves, we can compare with Eq. 2. This analysis is shown in Fig. 4. We also note a decrease in amplitude at around 1257 Oe, which we believe is due to the edges of our sample not being parallel.

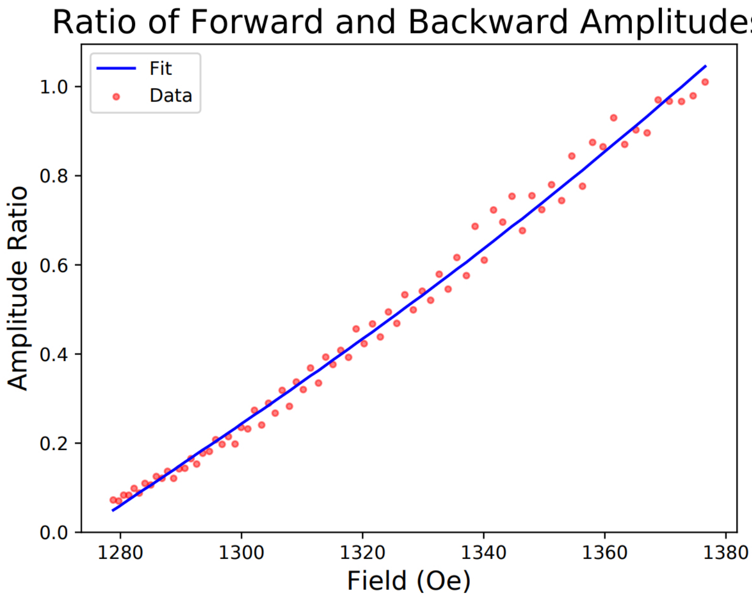

Fig. 4. A plot of the ratio of amplitudes of the forward and backward propagating spin waves as a function of field, as plotted in Fig. 3. Comparing these amplitudes to Eq. 2 we can fit for the magnitude of the DMI parameter, which we find to be $D = -5.69 \times 10^{-4} \pm 0.05 \times 10^{-4}$ mJ / m^2. If we assume this is the sole mechanism of forward/backward amplitude asymmetry, then this value places a limit on the magnitude of the DMI parameter in this YIG / GGG system.